Marek STEMBALSKI[1*]
Pawel PRES[2]
Waclaw SKOCZYNSKI[1]
Paweł TUREK[1]

MODELLING OF A GLASS GATHERER ROBOT ARM
WITH A FRICTIONAL DAMPER

A numerical model of a friction damper used for damping vibration in glass gatherer robots was described. The damper with a lance was modelled using finite elements. Primary natural frequency of the system was determined. Numerical calculations were performed to determine the best operating parameters of the damper for excitations using a impulse of a force. Results of the damping decrement calculations for the friction damper model with a constant coefficient of friction and for the model, in which the coefficient of friction varied depending on the sliding velocity and the normal pressure occurring at the contact surfaces of the damper's friction rings, were presented. Based on numerical simulations, the values of relative displacements between the damper's friction rings were also determined

1. INTRODUCTION

The main task of glass gatherer robots, also referred to as ball gatherers, is moving molten glass from the furnace to the moulding device. The robot uses a lance with a ball on the end to directly transfer molten glass. Prior to the introduction of glass gatherer robots to glassworks, this work was performed by humans. However, the working conditions associated with the manufacture of glass products, such as high temperature emitted by the furnace, high levels of noise and monotony of operations performed, were relatively difficult for employees. Manual manufacture resulted in a significant amount of defects in products, as well as the deterioration of their quality. The use of glass gatherer robots in the manufacture of glass products brought certain advantages, such as the administration of precise amounts of molten glass in a short time, an increase in the homogeneity of the administered mass, a radical reduction of the amount of air bubbles in the glass, a better quality of products.

_____

[1] Wroclaw University of Technology, Department of Machine Tools and Mechanical Technologies, Wroclaw, Poland
[*] marek.stembalski@pwr.edu.pl
[2] Instytut Lotnictwa, Warszawa, Poland

During the process, the operation of the ball gatherer can be affected by excessive vibrations. These vibrations have a negative impact on the quality of products manufactured. They lead to an uneven distribution of the glass mass on the surface of the ball, and their occurrence when the material flows off the ball to the mould changes the thermal conditions of solidification of the material. The result is the formation of different kinds of defects on the surfaces of products, and thus deterioration of aesthetic values.

Research conducted the Wrocław University of Science and Technology [1–3] have shown that the most unfavourable vibrations from the point of view of the manufacturing process are associated with excitations induced by inertial forces of working units occurring during acceleration, braking and turns. Dynamic tests of the robot structure carried out in laboratory and industrial conditions have shown that the vibration spectrum is dominated by a single, relatively low frequency, which is associated with the local vibrating system. This system is the flexible lance with the ball. High flexibility of the lance results from its design. The lance has an axial hole for the transport of coolant. Furthermore, it has a large outreach necessary to collect the molten glass mass from the furnace.

Analysing a robot's operating cycle it can be observed that the greatest vibrations take place when the mass is gathered on the ball and fed into the mould. When the molten glass is gathered from the furnace, the vibrations are rapidly damped due to the consistency of molten glass, but may affect its uneven distribution on the surface of the ball. In contrast, during the transfer of the mass into the moulding device, vibrations are caused by inertial forces caused by stopping the lance with the ball above the mould. Their effect is an uneven filling of the mould and the formation of smudges on the surface of moulded glass products.

There are several ways to reduce the amplitude of vibration of the working unit. One of them is to increase the stiffness of the lance by reducing the size of the cooling hole, or by increasing the cross section of the lance. However, increasing the size of this section would result in an increase in the weight of the working unit, which in effect would not cause an increase of the fundamental frequency of natural vibration. Furthermore, this solution is associated with interference in the structural system of the ball gatherer.
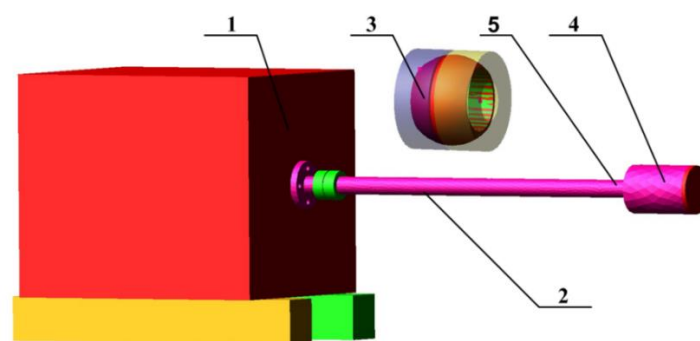

Fig. 1. Numerical model of a glass gatherer robot lance with a friction damper: 1 – cost iron block, 2 – lance, 3 – friction damper, 4 – equivalent weight, 5 – lance tip [5]

Another way of reducing value of the vibration of the lance is changing the method of control. This can be achieved by reducing the velocity and acceleration of individual

units of the robot. Additionally, smooth deceleration of the ball above the moulding device and smooth start at the place of gathering of the molten glass may be introduced. However, this is dependent on the capabilities of the control system. Each of the proposed solutions would involve a direct interference in the structure of the robot or the control system (replacement of the controller, drives). The last possible way of reducing the amplitude of vibration of the ball gatherer is the use of a damper mounted directly on the robot's lance. This solution with the use of friction damper is presented in the paper.

2. A FRICTION DAMPER FOR A GLASS GATHERER ROBOT ARM MODELLED IN MSC ADAMS

Implementation of a prototype laboratory model of a friction damper was preceded by the construction of a numerical model [4, 5] The robot lance with the fitted friction damper (Fig. 1) was modelled using MSC ADAMS 2005 r2 [6].

Simulations carried out showed that the numerical model is sensitive to the change of the contact parameters between the friction rings (such as contact stiffness, depth of penetration, the coefficient of static and dynamic friction). It was also shown that the presence of a friction damper increases the damping decrement of the glass gatherer robot's unit. The numerical model also features the optimal preload force of the damper rings, at which the system has the best damping properties. However, in the model, this force is more than two times larger than the force used in experiments. The damping decrement determined by numerical simulation was more than twice as large as that obtained from experiments.

As a result of the carried out simulations, it was found that the MSC ADAMS software environment has some limitations that prevent the modelling of contact between the friction damper rings. These limitations result from the fact that ADAMS does not allow for the implementation of a contact between two flexible elements of the flex type. The necessity of modelling damper rings using rigid components of the solid type represents a major simplification of the model. For this reason it was decided to change the software environment to ABAQUS.

In addition, coefficients of static and dynamic friction used in the calculation in the above-described numerical model came from the MSC ADAMS software documentation [6]. There was no certainty about the correctness of these values. For this reason, the coefficient of friction was determined empirically for the material from which the prototype friction damper was made, as described in [7].

3. NUMERICAL MODEL OF A GLASS GATHERER ROBOT'S ARM FITTED WITH A FRICTION DAMPER MADE IN THE ABAQUS CALCULATION SOFTWARE

The first step in the implementation of the numerical model was modelling the lance without the friction damper (Fig. 2). The described model has been simplified in comparison to the first simulations performed in MSC ADAMS environment. Modelling

of the iron block and sleepers was abandoned, so that the final model had a smaller number of components and numerical simulations were performed in a shorter time. The mounting flange, glass gatherer robot arm, the adapter and the equivalent weight were modelled together as a single part.
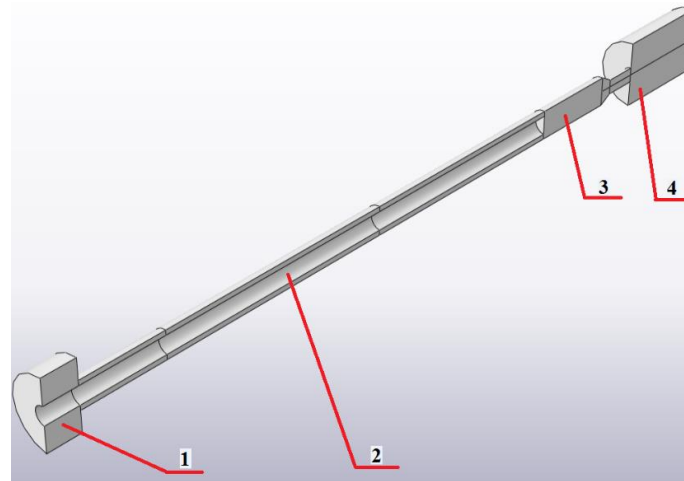

Fig. 2. Numerical model of the glass gatherer robot lance without a friction damper:
1) lance's mounting flange, 2) lance, 3) adapter, 4) equivalent weight

Partial validation of the numerical model was obtained by examining the fundamental natural frequencies of the lance in the numerical model and the physical model. The calculations were made for the lance itself, after which subsequent equivalent weights were added. The results of the calculation of fundamental frequency of natural vibration for different combinations of equivalent weights are shown in Fig. 3.
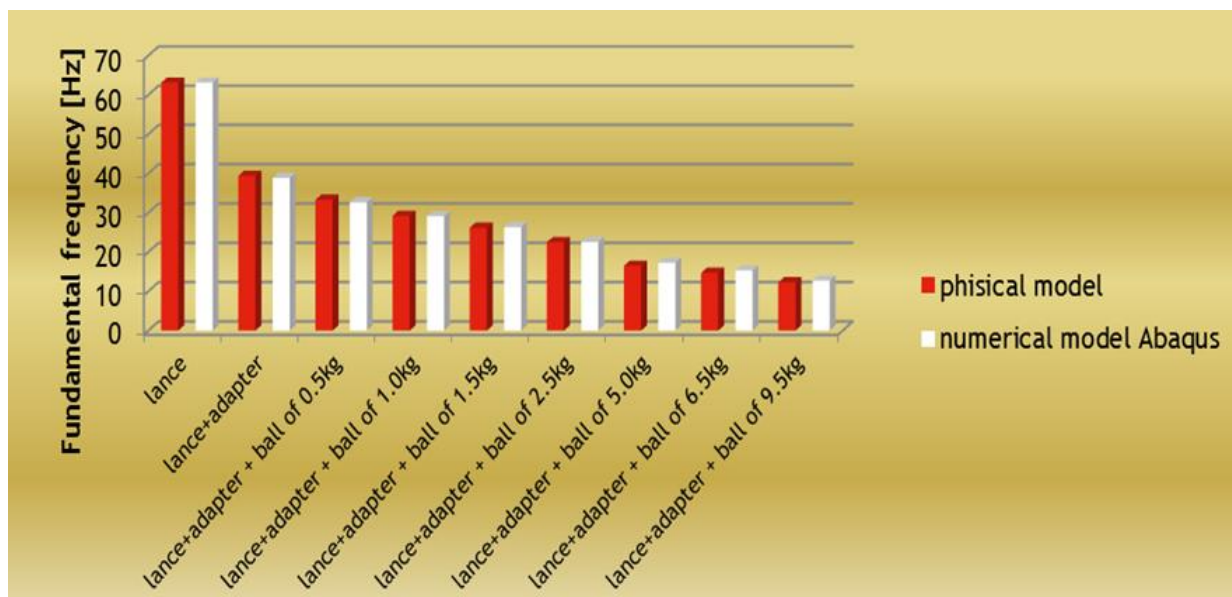

Fig. 3. Comparison of the fundamental frequencies of natural vibration in the numerical and the physical model of the lance for different equivalent weights

The results obtained on the basis of numerical calculations and dynamic tests of the physical model for fundamental frequency of natural vibration of the lance with different equivalent weights showed a high level of conformity. The biggest differences were found in the model of the lance with an adapter and a 5 kg equivalent weight. In this case, the numerical simulations showed frequency higher by 4% than that obtained in laboratory tests.

After calculating the fundamental frequency of natural vibration of the lance with equivalent weights attached, its damping has been determined. After the impulse of a force excitation of the the lance on the laboratory test stand, the logarithmic decrement was determined based on the characteristic of free vibration. Then, in the numerical model, using the Abaqus/Explicit package, Rayleigh coefficients were chosen so that the first 30 amplitudes coincided with the experimental results.
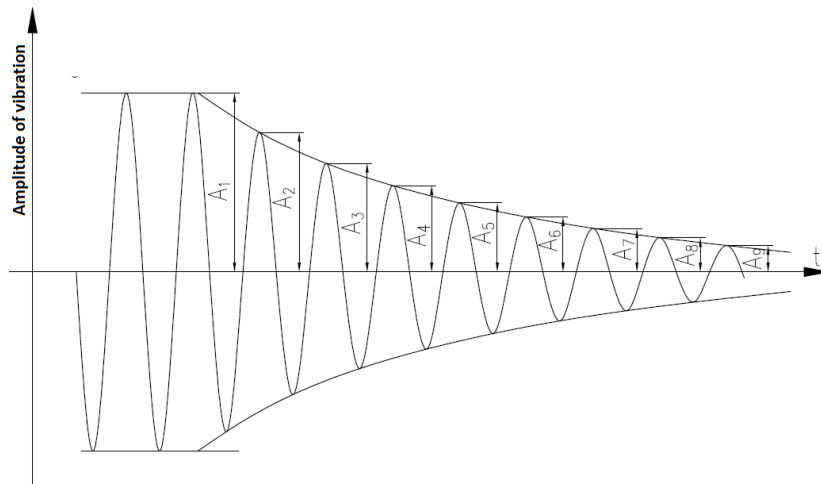

Fig. 4. Time course of damped vibration [8]

$$\delta_1 = \frac{1}{2}\ln\frac{A_1}{A_3}; \qquad \delta_2 = \frac{1}{2}\ln\frac{A_4}{A_6}; \qquad \delta_3 = \frac{1}{3}\ln\frac{A_6}{A_9};$$

$$\delta_4 = \frac{1}{5}\ln\frac{A_1}{A_6}; \qquad \delta_5 = \frac{1}{8}\ln\frac{A_1}{A_9} \tag{1}$$

The final value of the logarithmic damping decrement is determined by the arithmetic mean.

$$\delta = \frac{1}{5}(\delta_1 + \delta_2 + \delta_3 + \delta_4 + \delta_5) \tag{2}$$

The next step in the creation of a numerical model was modelling of the friction damper and necessary fasteners (Fig. 5). The modelled friction damper was supported on one side directly on the lance's mounting flange and on the other side was pressed against the thrust disc. Causing a displacement of the thrust disc along the axis of the lance made it possible to enter the preload force of the damper rings into the model. The principle of operation of the friction damper mounted on the lance of the glass robot is shown schematically in Fig. 6. The symbol *F* means the preload force of the damper rings.
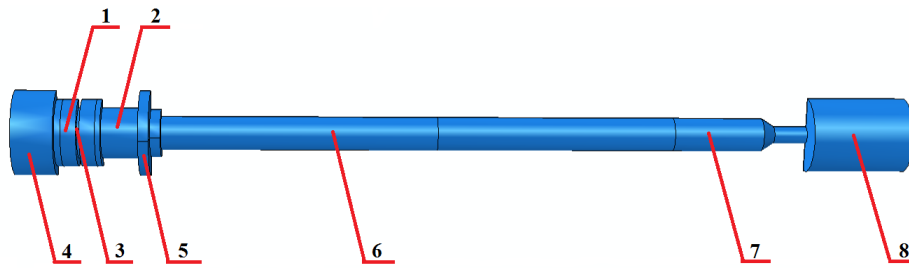
Fig. 5. Numerical model of a glass gatherer robot lance with a friction damper: 1) left outer friction ring, 2) right outer friction ring, 3) inner friction ring, 4) flange mounting the lance, 5) thrust disc, 6) glass gatherer robot's arm, 7) adapter, 8) equivalent weight
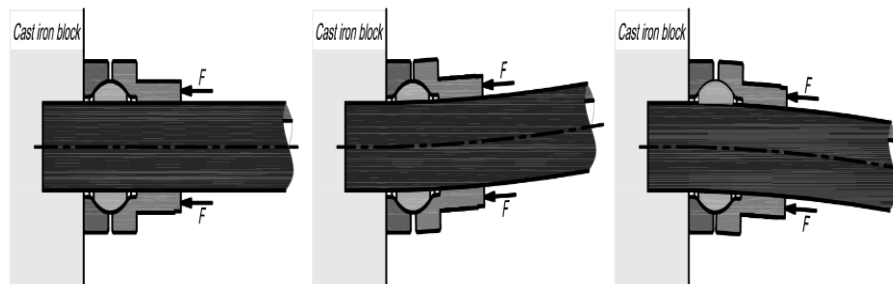

Fig. 6. Functional diagram of the friction damper during the deformation of the glass robot's lance

Friction damper consists of three rings: two external and one internal. During operation of the damper the cooperating rings are moved angularly relative to each other under the influence of different rotation angles of the lance cross-sections. Under the effect of excitation forces occurs some vibration, as a result of which the lance is deformed. This causes relative micro-slips of the rings. External rings perform rotary motions with respect to the transverse axis of the inner ring. As a result of the friction between the spherical surfaces of the damper's rings occurs energy dissipation reducing amplitude of the lance vibration.

During the manufacture of the damper's elements the biggest problem caused fitting friction surfaces. The damper had spherical surfaces whose diameter according to the design assumptions was 60 mm. In order to ensure a maximum damping efficiency the spherical friction surfaces should have the same radii of curvature and the lowest possible roughness so that the contact surface and thus the surface of cooperation was as large as possible. The appropriate roughness and similar radii of spherical surfaces curvature allow to obtain contact of mating surfaces close to the superficial. It is very important that the greater the contact area the damper's rings the higher the relative energy dissipation in structural connections.

Fig. 7 shows an exemplary course for changes in the value of the damping coefficient depending on increase the preload force of damper's rings. This course is obtained by modelling the lance with a friction damper. The model does not take into account the coefficient of friction as a function of the sliding velocity and the normal pressure, as described in [7]. It was assumed constant friction coefficient of 0.3. There was also not taken into account the weakening factor d_c [9]. The results shown in Fig.7 present the course of the damping coefficient for not optimized numerical model.
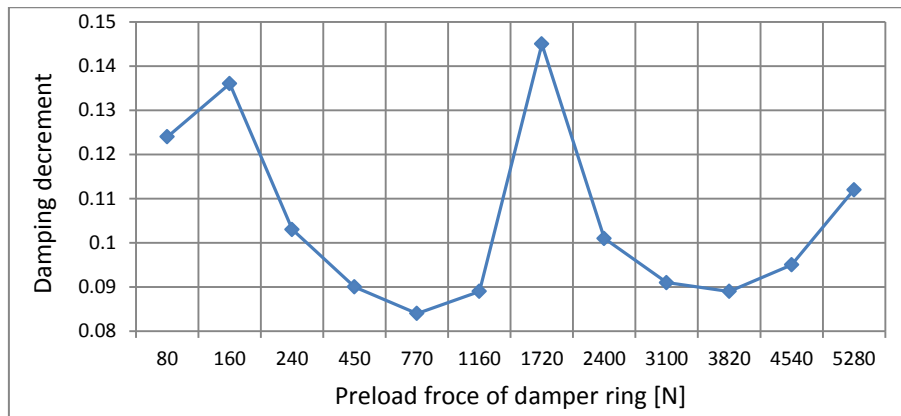
Fig. 7. Dependence between the damping decrement and the preload force of the friction damper rings - results of numerical simulations in model without optimization (with friction coefficient constant value)

The next step creation of a numerical model was the proper modelling of the contact between the mating friction parts, i.e. between the damper friction rings. For this purpose it was necessary to determine the effect of displacement of the thrust disc depending on the preload force of the damper rings. In order to do it, a friction damper was mounted on the lance along with a strain gauge dynamometer, a spacer ring and a thrust disc (Fig. 8). An inductive displacement sensor (1) was placed against the front surface of this disc (4). Then, the thrust disc was tightened and the value of preload force of the damper rings (2) was measured using a dynamometer (3).
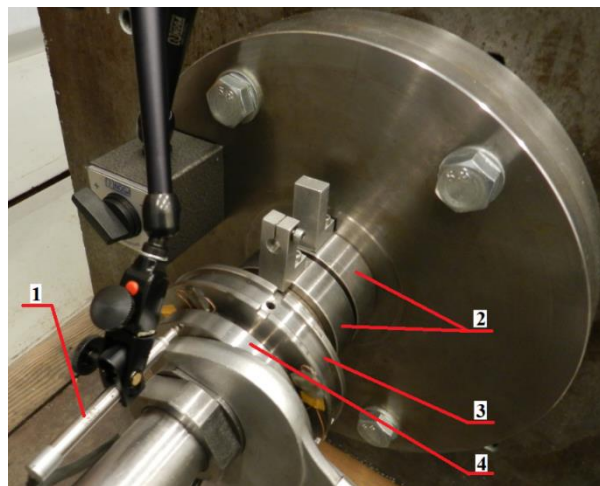

Fig. 8. Measurement of preload force depending on the displacement for the clamping disc: 1) inductive displacement sensor VIS MDKa-E1, 2) outer friction rings of the damper, 3) ring- shaped strain gauge dynamometer, 4) thrust disc

As a result of these tests, the displacement characteristic of the thrust disc depending on the set preload force of friction rings was determined (Fig. 9). The measurements were repeated five times. For each value of force, the average value of displacement was determined and standard deviation calculated. The relationship determined is non-linear and is characterised by relatively high standard deviation values, reaching, at low preload forces, up to 50% of the value of displacement. Then, the measured values of displacements and

preload forces were implemented in the Abaqus numerical software, thus obtaining the relationship between the displacement of the thrust disc and the preload force of the damper friction rings.
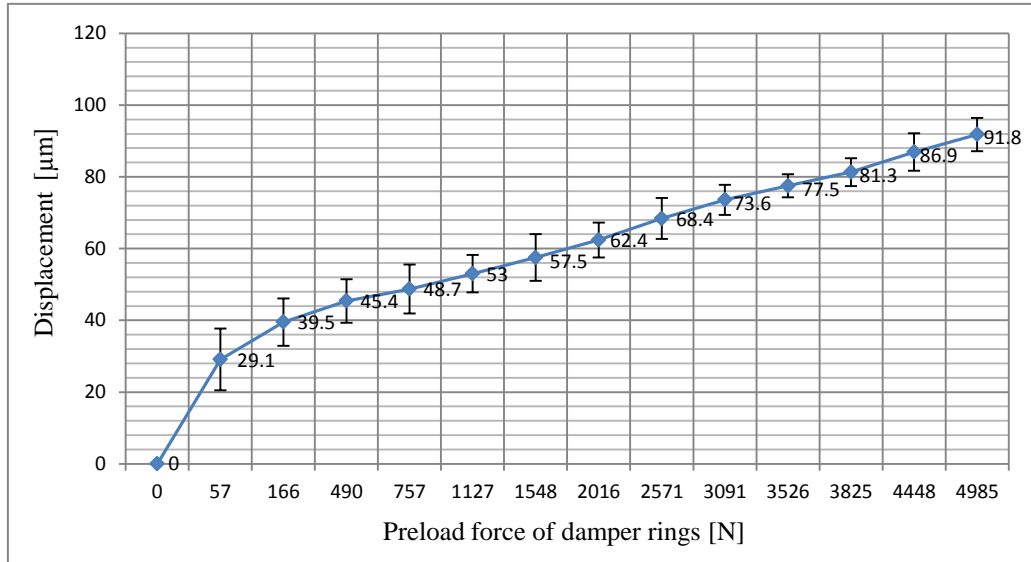

Fig. 9. Relative displacements of dampers rings, depending on the preload force of damper rings

In the ABAQUS calculation program, the value of the friction coefficient can be implemented in several ways, for example, by entering a single constant coefficient of friction. Another method is to factorize the constant value of the coefficient into the static friction coefficient μ_s and kinetic friction coefficient μ_k, whereas the value of the attenuation coefficient must also be specified d_c [9]. The values of friction coefficients reported in the literature for steel [6, 10–12] have a high discrepancy. There is also no certainty as to the specific value of the attenuation coefficient [12–15].

Therefore, in the described model it was decided to model the coefficient of friction as a function of normal stress and the sliding velocity.

Numerous experimental studies have shown that as the rubbing speed, the normal pressures, the temperature and other unspecified factors increase, the value of friction coefficient μ changes nonlinearly [16].Each material has its singular graph of function μ, which in a general form can be written as:

$$\mu = f(\rho, \dot{\gamma}, T, f^{\alpha}) \tag{3}$$

where:

ρ – normal pressure, $\dot{\gamma}$ – rubbing speed, T – temperature, f^{α} – other unspecified factors.

Knowing the curve of the friction coefficient versus the above variables one can more precisely predict the value of the tangent force and that of the dissipated energy, produced by friction between two bodies moving relative to each other.

Studies so far have shown that for most materials the friction coefficient at a rubbing speed equal to zero is higher than the one during sliding [17, 18]. This observation is expressed by an exponential model described by the following relation [9]:

$$\mu = \mu_k + (\mu_s - \mu_k)e^{-d_c\dot{\gamma}} \tag{4}$$

where:

μ_k – a coefficient of kinetic friction, μ_s – a coefficient of static friction,
d_c – a coefficient of attenuation.

However, in many cases the model with friction coefficient exponential attenuation is insufficient. Numerous studies [19, 20] have shown that the friction coefficient to a large extent depends on the normal pressures. The accuracy of friction force estimation increases when the normal load is taken into account.

Therefore the authors decided to make an attempt to determine the friction coefficient as a function of rubbing speed $\dot{\gamma}$ and normal pressure ρ in order to incorporate the derived relation into the numerical model of the passive friction damper.

A detailed description of the method of determining the damping coefficient as a function of sliding speed and normal pressure was presented by the authors in the [7]. As a result of the research, dependence was determined relation (5)

$$\mu = 0{,}2e^{-0{,}375\rho} + 0{,}046e^{(-(-1{,}84\ln(\rho)+8{,}42)\dot{\gamma})} \tag{5}$$

In the numerical model, the preload force of the damper rings was changed by setting the displacement of the mounting disc along the axis of the lance. The first step, the modelling disc was displaced by the set value, then the disc was blocked in several nodes thus preventing its withdrawal. The initial oscillations shown in Figures 10, 11, 12 in a time interval 0-0.3 s are caused by running the simulation model taking into account of gravity. During the numerical simulations exciting force was introduced by applying the force vector (a value of 93 N) to the equivalent weight located at the end of the lance. The force acted in the vertical axis direction in accordance with the gravity force. During the simulation vibration displacements of the lance tip were measured in the direction of the applied force vector (Fig. 12). Relative displacements occurring between the outer rings of the friction damper were also measured. Sample time series of preload force changes after excitation using a impulse of a force are shown in Fig. 10.

All elements of the numerical model were modelled using symmetry properties. This considerably reduced the duration of numerical simulations. For this reason, the value of the preload force of the friction damper rings, read from Fig. 10, should be multiplied by two. In all cases, the nature of the preload force waveforms is similar. In interpreting the results of simulation, the downforce values after its stabilisation were considered as appropriate (Fig. 10, time 0.5 s). Depending on the size of the initial movement of the thrust disc, a range of changes in the preload force from 90 N to 5360 N has been obtained. This range coincides with the forces used during laboratory tests.

In addition, taking into account the preload force, the displacement amplitudes of the relative vibrations of outer damper rings were measured. Sample time series of relative displacement changes after excitation using a impulse of a force are shown in Fig. 11.

On the basis of numerical simulations, it was found that at a minimum initial downforce (90 N), the largest amplitude of relative displacements of vibration the rings was 39 μm, and for the downforce used most often (5360 N), it amounted to 17 μm.
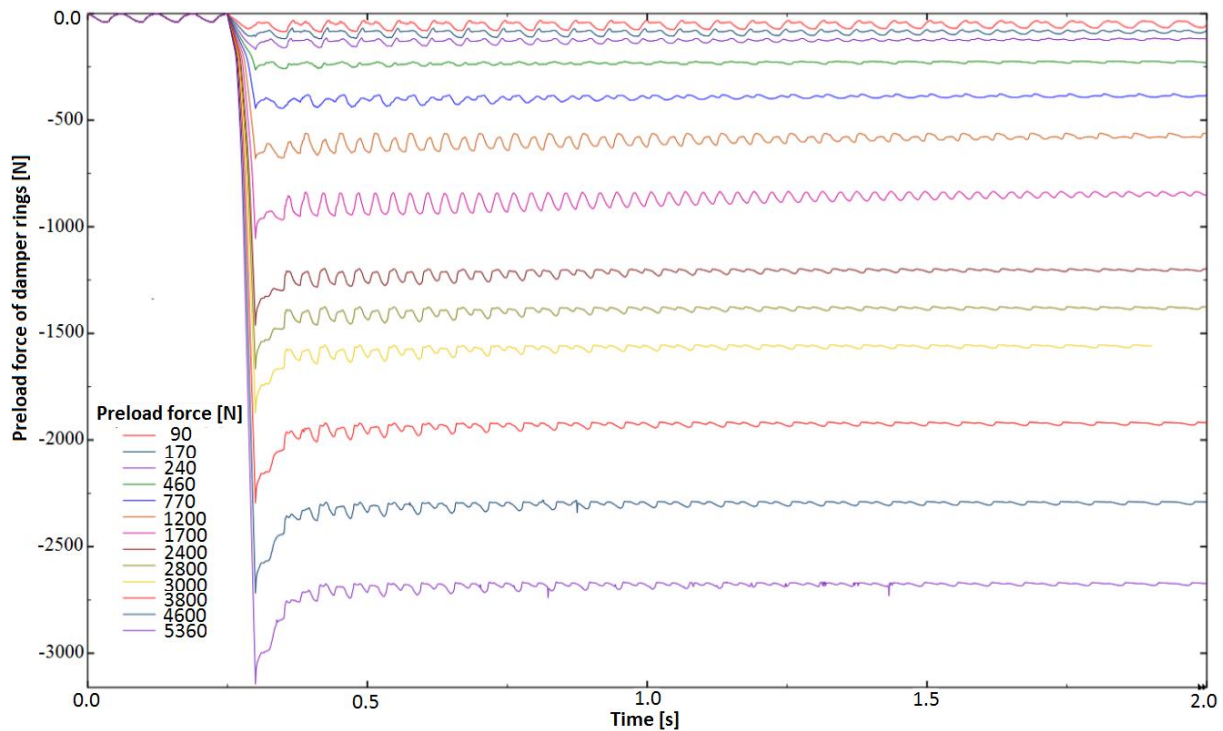
Fig. 10. Time series of damper ring preload force changes after excitation using an impulse of a force

During the experimental tests, the greatest amplitudes of the displacement of relative vibrations of the damper rings for initial downforce of 400 N amounted to 40 μm, while for the force of 5000 N, they amounted to 7 μm.

In addition, during the simulations, the static deflection of the lance and its vibrations in the vertical plane were determined. Figure 12 shows the graph of the displacement of the lance tip vibrations after excitation using a impulse of a force. In the first case, these are vibrations of the system without the damper, while in the second case – with the modelled friction damper.

Experimental studies carried out as a part of preliminary tests before creating the numerical model showed that up to a certain preload force the damping decrement value increases. During increasing this force rises the number of places where asperities of spherical rings are in contact. As a result of the external load contacting surfaces of the friction rings are moved relative to each other. About the work of friction forces in contact determines the number of places in which can occur micro-slip of asperities, friction forces and the length of the micro-slip distances. Energy dissipation in the damper is the sum of the elementary work of friction forces on the corresponding micro-slip distances in non-tacking contact areas. Above a certain value of the preload force some of contacting asperities undergoes tacking. A result of this is a reduction in the number of a potential micro-slip, thereby decreasing the work of friction forces. Therefore, it is important that the preload force of the friction damper was so adjusted as to obtain the best damping properties. With insufficient preload force can take place "opening a connection" causing as a result macro-slip in contact. Growing preload force leads to a gradual increase in the number of tacking asperities in contact and reduces the structural damping.
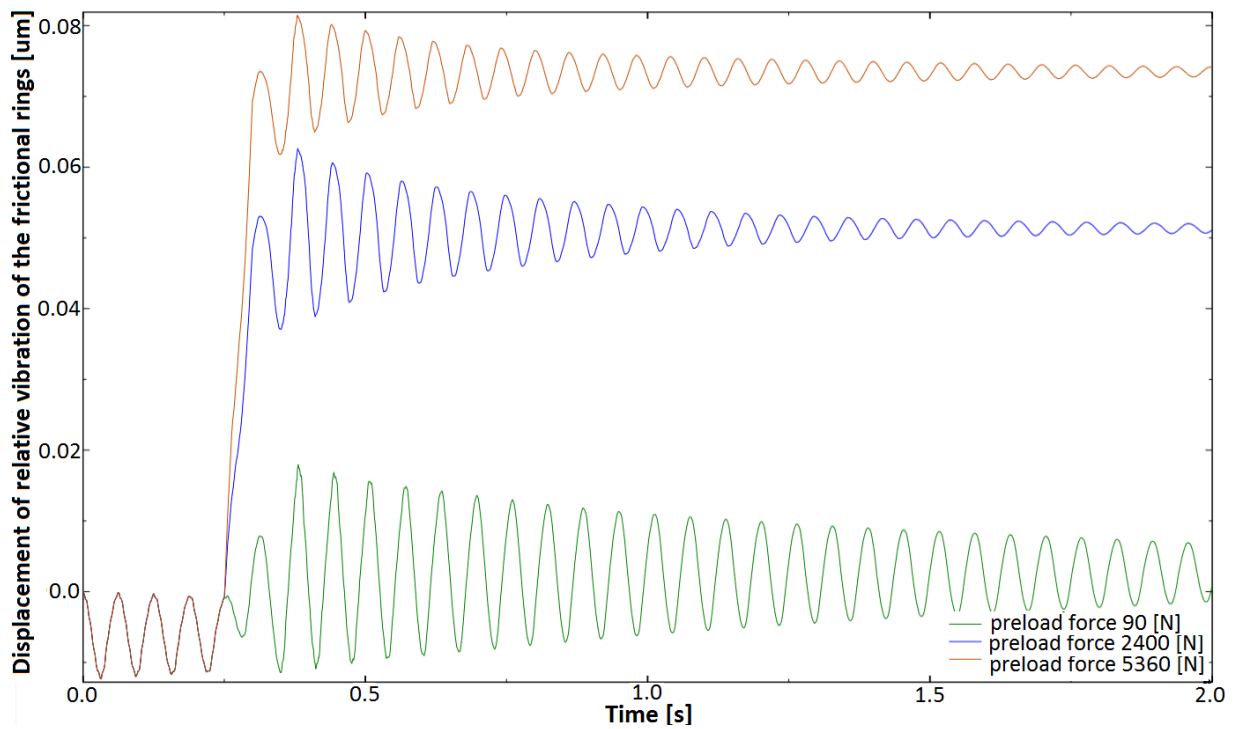
Fig. 11. Time series of the displacement of relative vibration of outer friction rings depending on the preload force
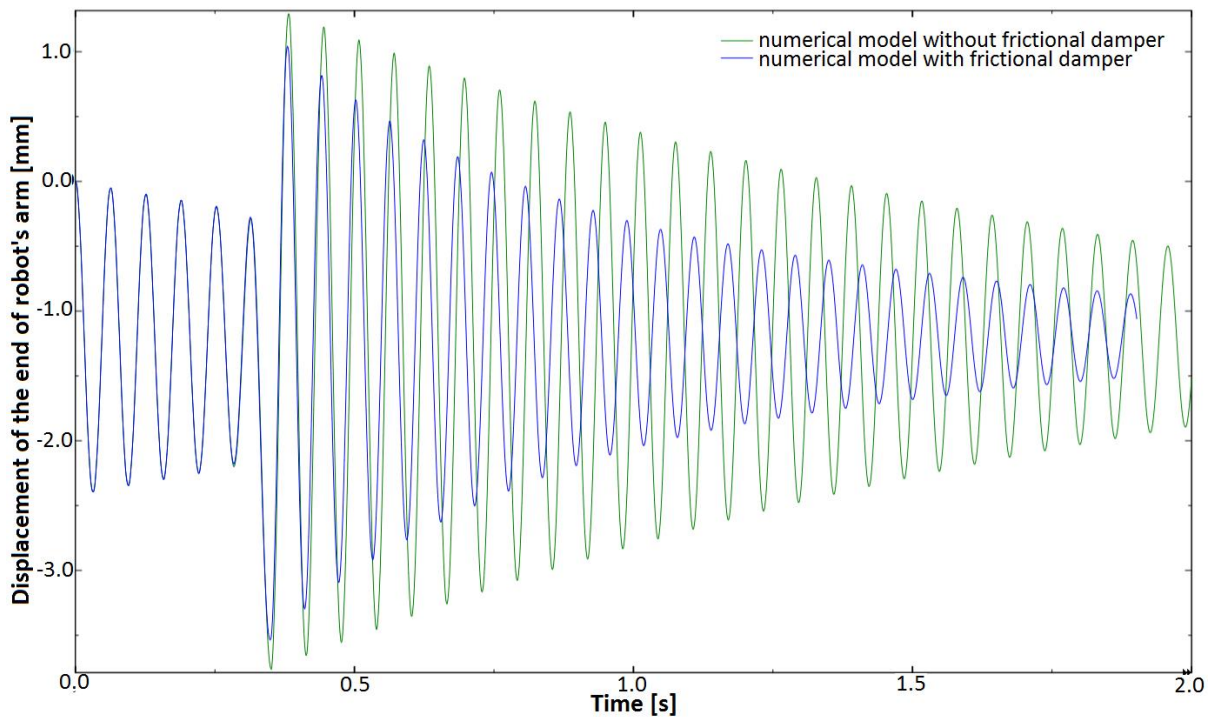

Fig. 12. Time series of the displacement of the lance tip vibrations after system excitation without the damper
and with the modelled friction damper for the preload force of 3000 N

Fig. 13 and 14 shows the dependence of damping decrement on the preload force of the damper's friction rings obtained after forcing using step function. Fig. 13 shows

the results of numerical calculations for model after the optimization using own developed coefficient of friction according to the equation described in [7]. While Fig. 14 shows course of damping decrement determined during experimental tests of physical model for step function excitations.

In the numerical model, as well as in the experimental tests, the average damping decrement was calculated on the basis of nine consecutive amplitudes. By analysing graphs 13 and 14, it should be noted that in both cases there is a clear maximum of the damping decrement values. It is the optimal preload force (for the numerical model it amounts to 3000 N, in the experimental tests it is equal to 1200 N) to be used to obtain the best damping properties of the system. Differences in estimated optimal preload forces may result from the failure to better estimate the displacement of the thrust disc depending on the preload force of the damper rings. In addition, in the numerical model based on the relationship specified (Fig. 9), displacement was determined in total in all the cooperating components of the damping system and the lance, i.e. the damper rings, damper rings with a lance, damper rings with the thrust disc. In reality, the displacements of the aforementioned cooperating components are different and depend on the type of connection and the nature of its operation. Numerical model of the damper does not include the gauge load cell as experimental studies of robot's lance damping was carried out without its presence. It was used only in a preliminary study of the physical model in order to measure the preload force between the damper's frictional rings.
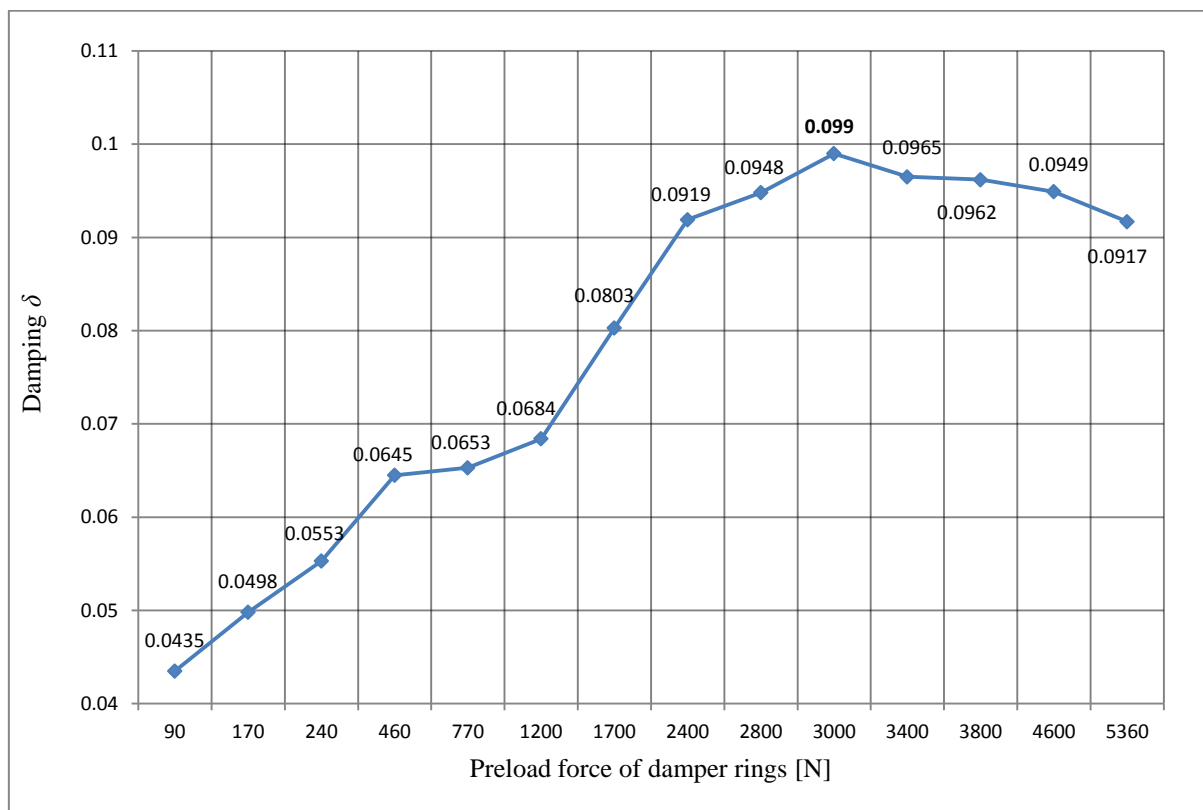

Fig. 13. Dependence between the damping decrement and the preload force of the friction damper rings obtained after excitation using a impulse of a force (93 N) – results of numerical simulations after optimization
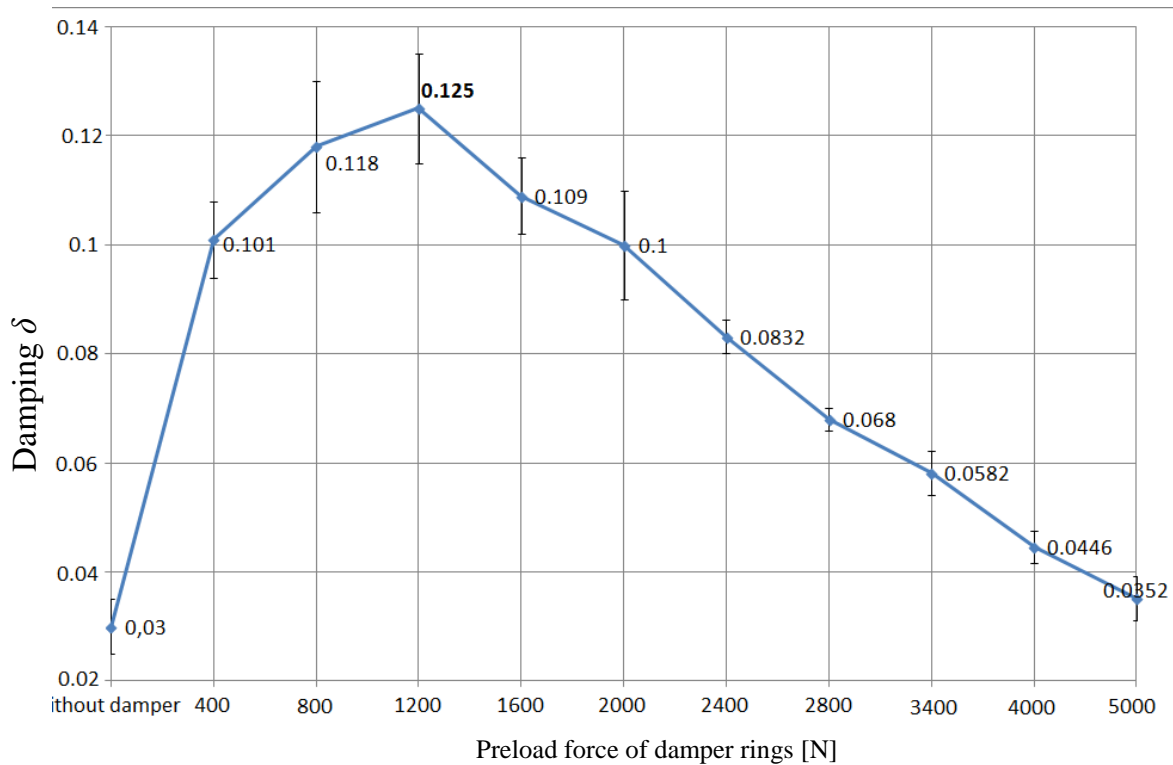
Fig. 14. Dependence between the damping decrement and the preload force of the friction damper rings obtained after excitation using a impulse of a force (93 N) – results of experimental tests

4. SUMMARY

Simulations carried out showed that the numerical model is sensitive to the change of the contact parameters between the friction damper rings and to the value of the exciting force acting on the lance. It was also shown that the presence of a friction damper increases the damping decrement of the glass gatherer robot's lance. Based on the tests carried out it should be noted that the maximum damping decrement determined in the numerical model is 20% smaller than one obtained in experimental tests. This may have its origin in a number of reasons, including the fact that the numerical model does not take into account the threaded connections between the lance and adapter as well as between the adapter and the equivalent weight. Also the connection of the lance with the iron block and its foundation on the sleepers were not modelled. These connections can cause an increase in the damping decrement in the laboratory stand.

In the numerical model, as well as in experimental tests, there is an optimal preload force at which the system has the best damping properties. In the numerical simulations, this force was more than twice the force determined by experiments. The reasons for this discrepancy should be sought in the inaccurate manner of determining the relationships between displacement of the thrust disc and the preload force of damper rings (Figure 9), and between the thrust disc, friction damper rings and the lance. The model also does not take into account the presence of the tensometric dynamometer and the threaded connection between the mounting disc and the lance. In addition, the estimated value of the displacement of the thrust disc was modelled equally to all mated connections, i.e. for the connection between the damper rings, the damper and the lance, as well as between the right outer ring and the thrust disc. In reality, relative displacement between the individual components of the damping system will be different. In addition, when we compare

graphs 13 and 7, it should be noted that the use of the dependence of the coefficient of friction on the sliding speed and normal pressures in numerical simulations resulted in the improvement of the quality of the numerical model.

REFERENCES

[1]   CHOROSZY T., MAREK B., ROSZKOWSKI A., SKOCZYŃSKI W., SZYMKOWSKI J., 2005, *Vibration measurement of glass gatherer robots during the implementation of the technological cycle*, Przegląd Mechaniczny, *LXIV/9,* 196–199, (in Polish).

[2]   SKOCZYŃSKI W., KRZYŻANOWSKI J., 2003, *Dynamic properties testing of glazier's robot structure, Modern trends in manufacturing*, Second International CAMT Conference, Wrocław 20-21 February 2003, PWr, Wrocław, 335–342.

[3]   SZYMKOWSKI J., SKOCZYŃSKI W., KRZYŻANOWSKI J., ROSZKOWSKI A., 2003, *Analysis of Glazier's Robot Structure Dynamic Behaviours*, Annals of DAAAM for 2003 & Proceedings of the 14th International DAAAM Symposium, Intelligent Manufacturing & Automation, Focus on Reconstruction and Development, Sarajevo, October 22–25, Vienna, 459–460.

[4]   STEMBALSKI M., SKOCZYŃSKI W., ROSZKOWSKI A., 2011*, Numerical model of friction damper for glass pick- up robot*, Techniki komputerowe w inżynierii, Bełchatów, 351–252.

[5]   STEMBALSKI M., SKOCZYŃSKI W., ROSZKOWSKI A., 2012, *Numerical model of frictional damper for glass – making robot lance*, Journal of Kones, 19/1, 391–398.

[6]   ADAMs User's Reference Manual, 2001, MDI, Michigan, USA.

[**7**]   STEMBALSKI M., PREŚ P., SKOCZYŃSKI W., 2013, *Determination of the friction coefficient as a function of sliding speed and normal pressure for steel C45 and steel 40HM*, Archives of Civil and Mechanical Engineering, 13/4, 444–448.

[8]   OSIŃSKI Z., 1997, *Damping of vibration*, Wydawnictwo Naukowe PWN, Warsaw, (in Polish).

[9]   Abaqus.6.9 software documentation.

[10] CRC Handbook of Physical Quantities, CRC Press. 1997, 145–156.

[11] LAWROWSKI Z., 2009, *Tribology – Friction, wear and lubrication*, Oficyna Wydawnicza Politechniki Wrocławskiej, Wrocław, (in Polish).

[12] CHEN M., KATO T., ADACHI K., 2002, *The comparison of sliding speed and normal load effect on friction coefficient of self-mated Si3N4 and SiC under water lubrication*, Tribology International, 35/3, 129–135.

[13] FEYZULLAHOGLE E., SAFFAG Z., 2008, *The tribological behavior of different engineering plastics under dry friction conditions*, Materials and Design, 29, 205–211.

[14] GRZESIK W., NIESŁONY P., 2004, *Prediction of friction and heat flow in machining incorporating therophisical properties of the coating-chip interface*, Wear 256/1–2, 108–117.

[15] SPIJKER P., ANCIAUX G., MOLINARI J., 2013, *Relation between roughness, temperature and dry sliding friction at the atomic scale*, Tribology International, 59, 222–229.

[16] KWIATKOWSKA E., 2008, *The influence of friction in fem simulation of chip formation*, Advances in Manufacturing Science and Technology, 32/2, 39–51.

[17] RECH J., CLAUDIN C., ERAMON E., 2009, *Identification of a friction model – Application to the context of dry cutting of an AISI 1045 annealed steel with a TiN-coated carbide tool*, Tribology International, 42, 738-744.

[18] TYAGI R., XIONG D., LI J., 2011, *Effect of load and sliding speed on friction and wear behaviour of silver/ h-BN containing Ni-base P/M composites*, Wear, 270, 423–430.

[19] YANG J., GU W., PAN L.M., SONG K., CHEN X., QUI T., 2011, *Friction and wear properties of in situ $(TiB_2+TiC)/Ti_3SiC_2$ composites*, Wear, 271, 2940–2946.

[20] ZEMZEMI F., RECH J., DOGUI A., KAPSTA P., 2009, *Identification of the friction model at tool/chip/ workpiece interfaces in dry machining of AISI4142 treated steel*, Journal of Materials Processing Technology, 209, 3978–3990.